Eur. Phys. J. D **30**, 5–9 (2004)
DOI: 10.1140/epjd/e2004-00050-2

THE EUROPEAN PHYSICAL JOURNAL D

Ionization of helium in positron collisions

I.F. Barna[a]

Max-Planck-Institute for the Physics of Complex Systems, Nöthnitzer Straße 38, 01187 Dresden, Germany

Received 26 November 2003 / Received in final form 18 February 2004
Published online 15 April 2004 –

Abstract. A new Coulomb distorted-wave method with coupled-channel target functions is used to calculate total ionization cross-sections for helium in positron collisions. Besides Slater-like orbitals we use regular Coulomb wave packets in our configurational interaction basis to describe the target continuum. The incident positron energy was varied between the ionization threshold and 500 a.u. The results are in good agreement with experimental data and other theoretical calculations. Comparing to other sophisticated distorted wave methods our model is much easier to implement and gives accurate results. As a new feature we present ionization cross-sections where the He^+ ion remains in the $1s$ ground state or excited to the $2s$ or $2p$ state. As we know there are no experimental work done to determine such cross-sections. In the case of ionization followed by $2s$ or $2p$ excitation we compared our results with other calculations.

PACS. 34.85.+x Positron scattering

1 Introduction

Ionization of helium in positron collisions has been extensively studied both theoretically and experimentally [1–5]. Positron-impact ionization calculations are simpler than electron-impact ionization calculations because there are no exchange effects. The first quantum-mechanical study of the ionization cross-section for positron impact of helium was carried out with the first order Born approximation using different kind of wave functions by [6]. The classical trajectory Monte-Carlo method agrees well with experimental data below 200 eV impact energy [7]. The time-dependent coupled-channel method was implemented with hyperbolic positron trajectories in the energy range 6−1000 eV by [8]. A much more elaborate coupled-channel method was presented in [9] including positronium formation. A distorted-wave method with close-coupled target states was developed to calculate total ionization cross-sections for noble gases in positron impact upto about 1 keV by [10]. Another distorted wave model was performed in the work of [11] and applied for noble gases also. Further details including references covering various methods are given in [9].

Here, we report on the new implementation of our coupled-channel method combined with Coulomb wave Born approximation for ionization of helium in positron collisions. So far, our original coupled-channel method has been successfully applied for time-dependent ionization processes such as heavy ion helium collisions to calculate total cross-sections [12,13] and for laser driven atomic processes in helium [14].

[a] e-mail: barna@mpipks-dresden.mpg.de

We take the electron-electron interaction fully into consideration which is important in single- and double-ionization processes. To represent bound states and resonances we use Slater-type orbitals. A special feature in our explicitly correlated basis are regular Coulomb wave packets, which we use to discretise the continua. As we will show, the low lying single- and double-Coulomb continua can be approximated well for positron ionization with the help of these wave packets. We use only single-centre expansion for the wave function and neglect positronium formation. To identify the double excited states embedded in the single electron continuum (e.g. $2s2s$) we adopted the method of complex scaling [15]. Atomic units are used throughout the paper unless otherwise indicated.

2 Theory

The centre-of-mass frame is used to describe positron impact on a helium atom. Our model is defined by the Hamiltonian

$$H = -\frac{1}{2}\nabla_p^2 + H_{\rm He} + V_{p-{\rm He}}. \tag{1}$$

The first term stands for the kinetic energy of the positron, $H_{\rm He}$ is the Hamiltonian of the unperturbed helium atom

$$\hat{H}_{\rm He} = \frac{\mathbf{p}_1^2}{2} + \frac{\mathbf{p}_2^2}{2} - \frac{2}{r_1} - \frac{2}{r_2} + \frac{1}{|\mathbf{r}_1 - \mathbf{r}_2|} \tag{2}$$

and $V_{p-{\rm He}}$ is the interaction operator between the positron and the target helium

$$V_{p-{\rm He}} = \frac{2}{R} - \frac{1}{|\mathbf{R} - \mathbf{r}_1|} - \frac{1}{|\mathbf{R} - \mathbf{r}_2|}. \tag{3}$$

$\mathbf{r}_1$, $\mathbf{r}_2$ and $\boldsymbol{R}$ are the coordinates of electrons 1 and 2 and the projectile positron with respect to the centre of mass, respectively. For the wave function we use the coupled-channel expansion

$$\Psi(\mathbf{r}_1, \mathbf{r}_2, \mathbf{R}) = \sum_n \varphi_n(\mathbf{R}) \Phi_n(\mathbf{r}_1, \mathbf{r}_2) \tag{4}$$

where the $\{\Phi_n(\mathbf{r}_1, \mathbf{r}_2)\}$ eigenfunctions are obtained by diagonalizing the time independent Schrödinger equation

$$\hat{H}_{\mathrm{He}} \Phi_n = E_n \Phi_n \tag{5}$$

in a basis of orthogonal symmetrized two-particle functions f_μ so that

$$\Phi_n(\mathbf{r}_1, \mathbf{r}_2) = \sum_\mu b_\mu^{[n]} f_\mu(\mathbf{r}_1, \mathbf{r}_2). \tag{6}$$

The choice of the single-particle functions will be specified later.

Substituting the total wave function (4) into the Schrödinger equation with the Hamiltonian (1) and projecting onto the helium channel wave functions $\Phi_n(\mathbf{r}_1, \mathbf{r}_2)$ gives the equations of motion

$$\left(-\frac{1}{2}\nabla_p^2 + \frac{2}{R} - \frac{k^2}{2} \right) \varphi_n(\mathbf{R}) + V_n(\mathbf{R}) \varphi_n(\mathbf{R}) = 0 \tag{7}$$

where

$$V_n(\mathbf{R}) = \left\langle \Phi_n(\mathbf{r}_1, \mathbf{r}_2) \left| -\frac{1}{|\mathbf{R} - \mathbf{r}_1|} - \frac{1}{|\mathbf{R} - \mathbf{r}_2|} \right| \Phi_n(\mathbf{r}_1, \mathbf{r}_2) \right\rangle \tag{8}$$

with the energy conservation

$$E_{tot} = E_{\mathrm{He}} + E_p = E_{\mathrm{He}} + \frac{k^2}{2}. \tag{9}$$

Equation (7) is to be solved with the following boundary condition, in the final channels as $\mathbf{R}$ goes to infinity:

$$\varphi_n(\mathbf{R}) \to f_n(\theta, \vartheta) \frac{e^{i(k_n R_n - \eta l_n 2 k_n R)}}{R} \tag{10}$$

where $\eta = \mu/k_0$ and $f_k(\theta, \vartheta)$ is the scattering amplitude in the channel n at angle (θ, ϑ) defined with respect to the direction of the incident momentum. Following Mott and Massey [16] and considering that the impact energy interval is larger than the threshold for singe-ionization, one may obtain the following expression for the differential cross-section:

$$\frac{d\sigma}{d\Omega} = |f_n(\theta, \vartheta)|^2 = \frac{4\pi^2 \mu^2 k_0}{k_n} \iiint d\mathbf{r}_1 d\mathbf{r}_2 d\mathbf{R} \times \sum_n \varphi_n^*(\mathbf{R}) \Psi_n^*(\mathbf{r}_1, \mathbf{r}_2) [\, V_{p-\mathrm{He}} - 2/R \,] \varphi_0(\mathbf{R}) \Psi_g(\mathbf{r}_1, \mathbf{r}_2) \tag{11}$$

where k_0 is the incident channel wavenumber and $\varphi_n^*(\mathbf{R})$ is the solution to the homogeneous part of (7) compatible with the asymptotic boundary condition (10) i.e. $\varphi_n^*(\mathbf{R})$ is the outgoing Coulomb wavefunction for positrons. For the $\varphi_0(\mathbf{R})$ initial positron wave function we take a plane wave with incident wavenumber k_0. The total ionization cross-section, σ^+, is obtained by integrating (11) over the solid angle $d\Omega$. For final states we sum over the possible n and, considering energy conservation (9). As initial helium state we take the ground state wave function $\Psi_g(\mathbf{r}_1, \mathbf{r}_2)$. This approximation helps us to take advantage of our continuum wave function built up from a large number of different configurations.

We now consider the helium channel wave function. In the following we restrict ourselves to singlet helium states only. For the single-particle wave functions we use an angular momentum representation with spherical harmonics $Y_{l,m}$, hydrogen-like radial Slater functions and radial regular Coulomb wave packets. The Slater function reads

$$S_{n,l,m,\kappa}(\mathbf{r}) = c(n, \kappa) r^{n-1} e^{-\kappa r} Y_{l,m}(\theta, \varphi) \tag{12}$$

where $c(n, \kappa)$ is the normalization constant. A regular Coulomb wave packet

$$C_{k,l,m,Z}(\mathbf{r}) = q(k, \Delta k) Y_{l,m}(\theta, \varphi) \int_{E_k - \Delta E_k/2}^{E_k + \Delta E_k/2} F_{k,l,Z}(r)\, dk \tag{13}$$

is constructed from radial Coulomb function of the well-known form [17]

$$F_{k,l,Z}(r) = \sqrt{\frac{2k}{\pi}} e^{\frac{\pi\eta}{2}} \frac{(2\rho)^l}{(2l+1)!} e^{-i\rho} \mid \Gamma(l + 1 - i\eta)| \times {}_1F_1(1 + l + i\eta, 2l + 2, 2i\rho), \tag{14}$$

where $\eta = Z/k$, $\rho = kr$ and $q(k, \Delta k)$ is the normalization constant.

The wave packets cover a small energy interval ΔE_k and thereby form a discrete representation of the continuum which can be incorporated into our finite basis set. The normalized Coulomb wave packets are calculated up to 315 a.u. radial distance or more to achieve a deviation of less then one percent from unity in their norm.

In our approach, two different effective charges Z have been used to take into account the difference between the singly- and the doubly-ionized electrons. For singly- and doubly-ionized states we used $Z = 1$ and $Z = 2$ respectively. A slight deviation from the effective charge gives practically no change in the final spectrum. We cover the single and double continuum up to energies of 10 a.u. equidistantly.

Out of the single particle states (12, 13) we have used 17 s-functions (9 Slater functions (sf), 4 wave packets (wp) with $Z = 1.0$ and 4 wp with $Z = 2.0$), 18 p-functions (6 sf, 6 wp with $Z = 1.0$ and 6 wp with $Z = 2.0$) and 12 d-functions (4 sf, 4 wp with $Z = 1.0$ and 4 wp $Z = 2.0$) to construct the symmetrized basis functions $f_\mu^{LM}(\mathbf{r}_1, \mathbf{r}_2)$. The non-orthogonality between the single-particle wave functions was taken fully into consideration throughout the diagonalization process.

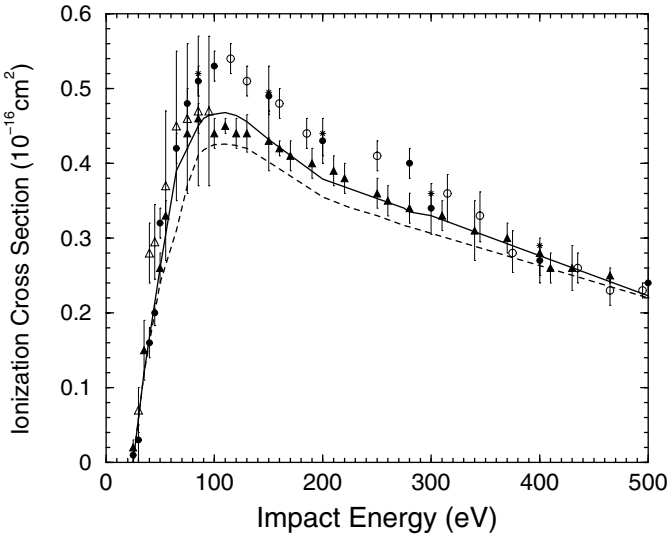

Fig. 1. Positron impact ionization cross-sections for helium. Experimental data: (•) Knudsen et al. [2]; (○) Moxom et al. [5]; (▲) Fromme et al. [1]; (△) Mori and Sueoka [3]; (∗) Jacobsen et al. [4]. The dashed line is from work of Campeanu et al. [11] and the solid line represents our calculations.

For the $L = 0$ configurations we have used $ss + pp + dd$ angular correlated wave functions to get a ground state energy of -2.901 a.u. which is reasonably accurate compared to the "exact" value of -2.903 a.u. For the $L = 1, 2$ states we have used only sp or sd configurations. The diagonalization process gives us 465 basis states up to 27 a.u. energy. Our results clearly demonstrate that the channels above 17 a.u. contribute very little to the ionization probabilities, which is anticipated from energy conservation. The maximum positron impact energy is 500 eV/27.2 eV = 18.38 a.u.

Between the first ionization threshold (-2.0 a.u.) and the lowest autoionizing bound state (-0.6931 a.u. for $L = 1$) our basis contains 22 states providing the major contribution for single ionization. Below the double-ionization threshold (0.0 a.u.), autoionizing bound states (such as $2s^2$) are embedded in the low-lying single-electron continuum. With the help of complex scaling these states can be identified and filtered out from the relevant ionization channels. The convergence checks of the calculations will be mentioned later. A detailed list of single- and double-excited states used in our calculation can be found in [14].

3 Results and discussion

To obtain the total cross-sections we solved equation (11) for 300 channels. The remaining $465 - 300 = 165$ channels correspond to excited and double-ionized states which do not contributes to single-ionization cross-sections. We compare our results for ionization in Figure 1 with the calculation of [11] and experimental data of [1–5] for positron impact energies between ionization threshold and 500 eV. Between the first ionization threshold (24.56 eV) and 50 eV our calculation is in good agreement with the experimental data and the results of [11]. Above this energy our theory gives larger cross-sections than the theory of [11]. Only at 500 eV impact energy our result agrees with [11] again. In the vicinity of 100 eV our theory exceeds even the experimental data of [1] by 5 percent and lies between the older [1] and newer measurements of [2, 5]. We explain these results with the large number of continuum states which we have in this energy range.

Campeanu [11] used his DCPE5 (distorted wave Coulomb plus plane waves with full energy range) modell [18] based on the prior form of the scattering T-matrix using the atomic static potential and a polarized-orbital polarization potential of [19]. In this model the final positron and ionized electrons are represented by free plane waves. We describe the ionized electron and the outgoing positron by Coulomb functions as we mentioned already.

After this basis-set test calculation we concentrated on ionization processes where the helium ion is in the ground state or simultaneously excited. We analysed the following reactions:

$$e^+ + \mathrm{He}(1s1s) \rightarrow \mathrm{He}^+(1s) + e^+ + e^- \qquad (15\mathrm{A})$$

$$e^+ + \mathrm{He}(1s1s) \rightarrow \mathrm{He}^+(2s) + e^+ + e^- \qquad (15\mathrm{B})$$

$$e^+ + \mathrm{He}(1s1s) \rightarrow \mathrm{He}^+(2p) + e^+ + e^- \qquad (15\mathrm{C})$$

where e^+ stands for positron and e^- for electron, respectively. In the first process the helium ion remains in its $1s$ ground state and the following two reactions include excitations. Figure 2 shows a comparison between our results and the calculations of Moores [10] for cross-sections obtained for simultaneous ionization and excitation of helium by positron impact (Eqs. (15B, 15C)), and our ionization cross-section results when the helium ion is not excited (Eq. (15A)).

The first ionization process (Eq. (15A)) gave us the largest cross-sections. This result meets our physical intuition saying that sate selective ionization without additional excitation has the largest cross-section. This cross-section is a factor of 24 larger than our predicted cross-section for $\mathrm{He}^+(2p)$ excitation and a factor of 40 large than for $\mathrm{He}^+(2s)$ excitation. To alleviate further comparisons our cross-section is $\sigma = 152 \times 10^{-19}$ cm^2 at 160 eV positron energy. This cross-section curve has a maxima in the vicinity of 110 eV and has a slow decay above this energy. Due to our knowledge there is no experimental or theoretical work available about this process.

For ionization with simultaneous excitation we compared our results with the work of Moores [10]. Our result predicts a cross-section $\sigma = 3.77 \times 10^{-19}$ cm^2 at 160 eV positron energy for simultaneous $\mathrm{He}^+(2s)$ excitation which is a factor of 5 larger than the prediction of [10]. For ionization escorted with $(2p)$ excitation our calculation exceeds the work of [10] by a factor of 4.4 at 160 eV positron energy giving $\sigma = 6.4 \times 10^{-19}$ cm^2. We explain our higher cross-section predictions with the detailed representation of the corresponding energy range.

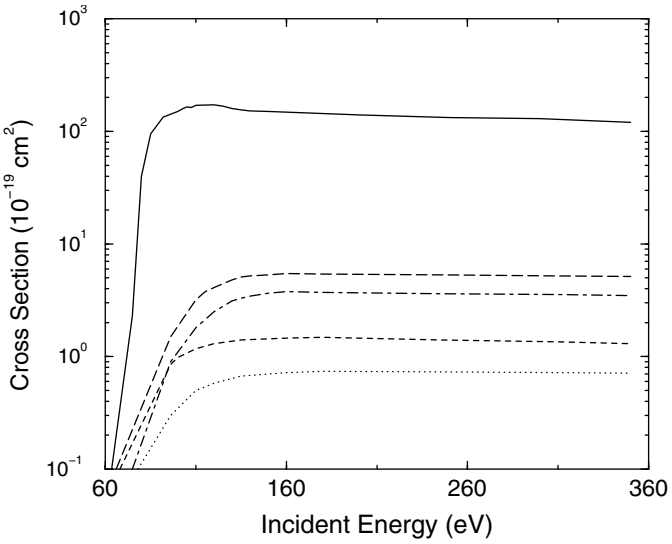

Fig. 2. Ionization cross-sections of helium in positron impact where the helium ion is in a well defined state. The three high lying curves represent our results, the solid line shows our results for equation (15A) process, long dashed curve for $He^+(2p)$ and the dash-dot-dashed is for $He^+(2s)$ simultaneous excitation. The dotted line shows the results of Moores [10] for ionization and $He^+(2s)$ excitation (Eq. (15B)), the short dashed curve is Moores [10] calculation for ionization and $He^+(2p)$ excitation (Eq. (15C)).

To check the convergence in the last three calculations is essential. We solved the eigenvalue equation through the complex scaling an filtered out the rotating continua from bound states and resonances. All the single-ionization states lie on different straight lines which have one end on the real axis. This end point is the energy value of the ionized helium atom e.g. $He^+(2s)$. With this method we know all the three different helium states $He^+(1s)$, $He^+(2s)$ and $He^+(2p)$ which we need. Another independent method is to investigate the helium electron densities and check the first maxima of the density. The position of this maximum shows us the radius of the bound electron orbital which is different for the $1s$ and the $2s$ states. Such electron densities can be found in [13][1]. These two independent methods gave us the same result.

To calculate the cross-sections we solved equation (11) with real eigenvalues and wave functions, the complex scaling only helped us to identify the states. We took more and more states into to sum of equation (11) till we reached convergence. Our result demonstrated that states where the ionized electron has more energy than the incident energy of the positron does not contribute to the sum, which is anticipated from energy conservation.

Moores [10] applied a sophisticated distorted-wave method with close-coupled target states and needed three different ab initio computer codes running on a supercomputer to get his results. More technical details can be found in [20].

[1] The cited densities are on pages 42 and 43.

Unfortunately there are no experimental data for these last two processes. We hope that our work together with [10] will stimulate experiments.

4 Summary

We have presented Coulomb distorted wave Born approximation calculations with coupled-channel helium target states for ionization of helium in positron impact. The channel functions were built up by Slater functions mainly to describe the bound states and regular Coulomb wave packets we use to approximate the continua. The incident positron energy was taken between the ionization threshold and 500 a.u. The accuracy achieved is excellent compared to experimental data and other theory. Due to our Coulomb wave packet basis we can approximate the helium soft electron continuum in detail, and reach cross-sections larger than another more sophisticated distorted-wave model [9]. Our method is easy to implement and does not need enormous computer capacity such as [10]. At some energies our results are even 5 percent higher than old experimental data.

Three different partial ionization cross-section calculations are presented also. For ionization without target excitation, (the He^+ ion remains in the $1s$ ground state) no theoretical or experimental work was done till now. Ionization with simultaneous target excitation was also examined and compared to another distorted-wave calculations. Our results are a factor of 4.4 larger for ionization He^+ and $(2s)$ excitation than the results of Moores [10]. For ionization and $(2p)$ excitation we got cross-sections which are a factor of 5 higher than Moores cross-sections. As explanation we emphasise the necessity of detailed approximation of the soft Coulomb continuum.

The motivation for this work was to test and show the validity of our coupled-channel helium states in positron helium ionization. This kind of coupled-channel basis set was successfully used in heavy-ion helium impact ionization and photoionization earlier. As a final summary about our three ionization study we may state that the proper treating of the soft coulomb continuum is essential. Further studies such as laser-assisted positron collisions are in progress.

References

1. D. Fromme, G. Kruse, W. Raith, G. Sinapius, Phys. Rev. Lett. **57**, 3031 (1986)
2. H. Knudsen, L. Brun-Nielsen, M. Charlton, M.R. Poulsen, J. Phys. B: At. Mol. Opt. Phys. **23**, 3955 (1990)
3. S. Mori, O. Sueoka, J. Phys B: At. Mol. Opt. Phys. **27**, 4349 (1994)
4. M.F. Jacobsen, N.P. Frandsen, H. Knudsen, U. Mikkelson, D.M. Schrader, J. Phys. B: At. Mol. Opt. Phys. **28**, 4691 (1995)
5. J. Moxom, P. Ashley, G. Lariccia, Can. J. Phys. **74**, 367 (1996)

6. M. Basu, P.S. Mazumdar, A.S. Ghosh, J. Phys. B: At. Mol. Opt. Phys. **18**, 369 (1985)
7. P.R. Schultz, R.E. Olson, Phys. Rev A. **38**, 1866 (1988)
8. Z. Chen, A.Z. Msezane, Phys. Rev. A **49**, 1752 (1993)
9. C.P. Campbell, M.T. McAlinden, A.A. Keroghan, H.R.J. Walters, Nucl. Instrum. Meth. B **143**, 41 (1998)
10. L.D. Moores, Nucl. Instrum. Meth. B **179**, 316 (2001)
11. R.I. Campeanu, R.P. McEachron, A.D. Stauffer, Nucl. Instrum. Meth. B **192**, 146 (2002)
12. I.F. Barna, N. Grün, W. Scheid, Eur. Phys. J. D **25**, 239 (2003)
13. I.F. Barna, Doctoral thesis, University Giessen (2002); `http://geb.uni-giessen.de/geb/volltexte/2003/1036`
14. I.F. Barna, J.M. Rost, Eur. Phys. J. D **27**, 287 (2003)
15. N. Moiseyev, Phys. Rep. **302**, 211 (1998)
16. N.F. Mott, H.S.W. Massey, *The Theory of Atomic Collision*, 3rd edn. (Clarendon, Oxford, 1965)
17. M. Abramowitz, A. Stegun, *Handbook of Mathematical Functions* (Dover Publications Inc., New York, 1972)
18. R.I. Campeanu, R.P. McEachran, A.D. Stauffer, Can. J. Phys. **77**, 769 (1999)
19. R.P. McEachran, D.L. Morgan, A.G. Ryman, A.D. Stauffer, J. Phys. B **10**, 663 (1977)
20. L.D. Moores, Nucl. Instrum. Meth. B **143**, 105 (1998)